Tay, D., McIntyre, D. L., & McDonald, J. J. (in press). Searching for visual singletons without a feature to guide attention. *Journal of Cognitive Neuroscience*. https://doi.org/10.1162/jocn_a_01890

Title: Searching for visual singletons without a feature to guide attention

Abbreviated title: Searching for singletons

Daniel Tay, David L. McIntyre, and John J. McDonald

Department of Psychology, Simon Fraser University, Burnaby, BC, Canada, V5A 1S6

*Corresponding author's Email: daniel_tay@sfu.ca

Abstract

Reaction-time studies have provided evidence for a singleton-detection strategy that is used to search for salient targets when there is no additional featural knowledge that would help guide attention. Despite this behavioural evidence, there have been few event-related potential (ERP) studies of singleton detection mode because it was reported early on that the ERP signature of attentional selection (the N2pc) is absent without feature guidance. Recently, however, it was discovered that a small and relatively late N2pc occurs in singleton detection mode along with a previously unreported component called the singleton detection positivity (SDP). Here we show that both components are influenced by the number of items in the display, as one might expect in a salience-based search mode. Specifically, the N2pc and SDP were larger when the set size was increased to make the singleton “pop out” more easily, when participants responded more quickly regardless of set size, and when RT search slopes were negative (Experiment 1). The latency of the SDP also depended on set size. In Experiment 2, EEG was recorded with a higher density electrode array to better characterize the scalp topography of the components and to estimate their neural sources. Regional sources near the ventral surface of extrastriate cortex in the occipital lobe explained over 96% of N2pc and SDP activities. These results indicate that searching in singleton detection mode selectively modulates processing within perceptual regions of visual cortex.

Keywords: visual search, singleton detection mode, event-related potentials, N2pc, SDP

Introduction

In a visual search task, an individual attempts to find an object of interest (target) that appears concurrently with other task-irrelevant items (nontargets). Stimulus processing during such search tasks has been theorized to involve early “preattentive” stages (Desimone & Duncan, 1995; Itti & Koch, 2000, 2001; Julesz, 1986; Neisser, 1967; Theeuwes, 2010; Treisman & Gelade, 1980; Wolfe, 1994), wherein stimulus information across the visual field is processed in parallel, and later attentive stages, wherein the features of a subset of items are processed selectively for identification or some other higher-level goal. The ease with which the target can be found depends on numerous factors, including its physical distinctiveness and the temporal stability of its features (e.g., Bravo & Nakayama, 1992). When its features are known in advance, attention can be guided with the aid of a target template stored in working memory (when features change from trial to trial; Bundesen, 1990; Chelazzi, Duncan, Miller, & Desimone, 1998; Chelazzi, Miller, Duncan, & Desimone, 1993; Desimone & Duncan, 1995; Duncan & Humphreys, 1989) or long-term memory (when features are fixed; Carlisle, Arita, Pardo, & Woodman, 2011; Logan, 1988; Woodman, Luck, & Schall, 2007). The search template can contain target features that will bias attention toward objects that resemble the target as well as features of known nontargets that might disrupt search if not suppressed or otherwise ignored (these to-be-ignored features may be stored in a separate template for rejection). In contrast, when the target’s features change unpredictably across time (as in a variable-mapping procedure; Schneider & Shiffrin, 1977), such feature-based guidance is not possible, and observers have to rely on other strategies to search for the target. If the target happens to be especially salient but otherwise unpredictable, an observer may adopt a strategy to search based solely on salience, using a mental map of visual salience that is constructed during the preattentive stage of processing. This particular search strategy has been labelled singleton detection mode to contrast it with the more typical feature-guided search mode (Bacon & Egeth, 1994).

The distinction between feature search mode and singleton detection mode was made explicitly to account for apparent inconsistencies in seminal studies of visual attention capture (Bacon & Egeth, 1994). Some of the seminal studies demonstrated that observers can ignore

salient distractors when they possess none of the defining features of the target (e.g., Folk, Remington, & Johnston, 1992), whereas others demonstrated that salient distractors defined in a completely irrelevant dimension (e.g., colour, when the target is a form singleton) impair target processing as if observers attended the distractor first and then redirected attention to the target (Theeuwes, 1991, 1992). Bacon and Egeth hypothesized that salience-driven distraction occurred in the latter studies because participants had adopted a singleton detection mode that ultimately biased attention toward the more salient singleton. In line with this hypothesis, they showed that a colour-singleton distractor delayed search for a concurrent fixed-feature target only when singleton detection mode could be adopted (that is, when the target was the only form singleton in the display). Critically, no delay was evident when participants had to rely on a feature-based strategy to find the target (that is, when the target was one of several form singletons in the display). A subsequent study showed that advanced training of a specific search mode determines whether salience-driven distraction occurs when searching for a fixed-feature target singleton, because either mode can be used under such conditions (Leber & Egeth, 2006). Such findings provide compelling behavioural evidence for a singleton detection mode that is based largely on bottom-up processing of stimulus salience and a feature search mode that guides attention using a target template stored in memory.

Electrophysiological studies of visual search have focused on an event-related potential (ERP) component called the posterior-contralateral N2 (N2pc; Luck & Hillyard, 1994a, 1994b). The N2pc is a negative-going potential over the posterior scalp that is isolated by comparing waveforms recorded from electrodes positioned contralaterally and ipsilaterally with respect to a presumably attended object or group of objects (for a review, see Luck, 2012). As its name suggests, the N2pc appears as a negative voltage in the contralateral waveform that occurs generally within the time range of the N2 peak (~170–300 ms). The N2pc can be observed in challenging search tasks wherein the target does not pop out from the display immediately (e.g., Luck & Hillyard, 1990; Dowdall, Luczak, & Tata, 2012), but it is typically studied using fixed-feature target singletons that are easy to locate. Consequently, the N2pc as an ERP signature of attentional selection has greatly contributed to our understanding of feature-guided visual search.

Although the ERP correlates of feature-search tasks have been the focus of intense investigation, the ERP correlates of singleton search mode were largely neglected until recently. This is because most ERP studies of visual search have focused on the N2pc, and the results of one early study indicated that the N2pc does not occur in singleton detection mode (Luck & Hillyard, 1994b, Experiment 2). In this experiment, observers searched eight-item displays for an orientation singleton (the target) that was present on half of the trials. The orientations of the nontargets changed randomly from horizontal to vertical, and thus the target and nontarget orientations swapped randomly across target-present trials. This variable-mapping procedure made it impossible for observers to engage in feature search mode, and thus, they had to employ a singleton-detection strategy. No N2pc was evident in their singleton-detection experiment, which indicated that the N2pc is present only when feature-guided search was possible. In most subsequent ERP studies of visual search, researchers allowed for feature search mode (e.g., by using consistent-mapping conditions) or feature discrimination (e.g., by using compound-search tasks; Duncan, 1985) so that the N2pc could be measured reliably (e.g., Burra & Kerzel, 2013; Hickey, McDonald, Theeuwes, 2006; Hickey, Olivers, Meeter, & Theeuwes, 2011; McDonald, Green, Jannati, & Di Lollo, 2013; van Moorselaar, Daneshtalab, & Slagter, 2021).

The absence of N2pc in Luck and Hillyard's (1994b) singleton-detection experiment has had substantial impact on our conceptualization of visual search and on the N2pc itself. However, growing evidence indicates that target singletons do elicit the N2pc in singleton detection mode (e.g., Mazza, Turatto, Caramazza, 2009a; Schubö, Schröger, & Meinecke, 2004; Tay, Harms, Hillyard, & McDonald, 2019; Tay, Jannati, Green, & McDonald, 2022). A small-but-significant N2pc was found using eight-item displays resembling those used by Luck and Hillyard (1994b), except that this N2pc occurred later than the conventional time window used to measure N2pc (250–350 ms; Tay et al., 2019). Larger and earlier N2pc components were found when larger set sizes were used (Mazza et al., 2009a; Schubö et al., 2004), suggesting that salience of the target determines the timing and amplitude of the "singleton detection N2pc". Besides the N2pc, two studies reported that singleton-present displays trigger a bilateral posterior positivity starting ~50 ms before the N2pc (Tay et al., 2019; Tay et al., 2022). The timing of this *singleton detection*

positivity (SDP) tracked the speed with which participants responded to singletons (Tay et al., 2019) and was nearly absent when display contained irrelevant-colour items (no-go trials; Tay et al., 2022). Given the original rationale for Luck and Hillyard's singleton-detection experiment, these new findings suggest that N2pc and SDP can be observed in the absence of feature guidance (see the General Discussion for consideration of the various ideas about what neuro-cognitive process causes the N2pc).

The aims of the present study were to determine how salience affects the ERP correlates of singleton detection mode (Experiment 1) and to estimate the neural sources of these ERP correlates (Experiment 2). In Experiment 1, the target's salience was varied across trials by randomly intermixing eight-item search displays with 12- and 16-item displays (**Figure 1**). Larger set sizes were not used to avoid a potential shift from a visual search mode to a separate *texture segmentation mode* (Sagi & Julesz, 1987, Schubö et al., 2004; Wolfe, 1992). The twin assumptions of Experiment 1 were that, in singleton detection mode, (1) the timing and amplitude of the N2pc (and possibly the SDP) depend on the ease with which the singleton "pops out" from the nontargets, and (2) the ease with which the target pops out is influenced by the number of items in the display (and/or the inter-item distances). Based on these assumptions, we predicted larger (and perhaps earlier) N2pc and SDP components would be associated with larger set sizes and shorter response times (RTs). In Experiment 2, a 64-channel electrode array was used to better characterize the scalp topographies of the SDP and the singleton-detection N2pc and to estimate the loci of their neural sources using a discrete-dipole approach. The goal was not to pinpoint the neural sources but to determine whether each component might arise from visual cortex. Prior MEG studies have sourced the magnetic equivalent of the N2pc to visual regions of the occipital and temporal lobes (Hopf et al., 2000), but the neural sources of the SDP have not been studied previously.

---------- Insert Figure 1 about here ----------

Experiment 1

Materials and Methods

The Research Ethics Board at Simon Fraser University approved the research protocol used in this study.

Participants

Fifty-seven students from Simon Fraser University without history of neurological disorders participated after giving informed consent. For their participation, students received either course credit as part of a departmental research participation system or $20. All students reported normal or corrected-to-normal colour vision using Ishihara color plates prior to participation. Data from seven participants were excluded from further analyses because more than 30% of their trials were contaminated by ocular artifacts (rejection criterion set in advance). Of the remaining 50 participants (mean age: 19.5 years), 29 were female and 46 were right-handed. The sample size of the present experiment was predetermined to have sufficient power (.80) to detect moderately small ERP effects (d = 0.40) because we expected, at minimum, a moderately small N2pc in 8-item displays and moderate increases in N2pc amplitude with increases in set size.

Apparatus

Experiment 1 was conducted in an electrically shielded and sound-attenuated chamber dimly illuminated by DC-powered LED lighting. Visual stimuli were presented on a height-adjustable, 23-inch LCD monitor running at 120 Hz. Participants sat in a chair and viewed the monitor from a distance of approximately 57 cm and made their responded using a gamepad. A Windows-based computer controlled stimulus presentation and registered participants' button presses using Presentation (Neurobehavioral Systems, Inc., Albany, CA). EEG was recorded using custom software (Acquire) from a second Windows-based computer, using a 64-channel A-to-D board (PCI 6071e, National Instruments, Austin, TX) connected to an EEG amplifier system with an input impedance of 1 GΩ (SA instruments, San Diego, CA).

Stimuli and Procedure

Each stimulus display contained a small, white fixation cross (0.3° × 0.3°; 0.3 cd/m^2) at the centre of the screen and 8, 12, or 16 cyan lines (0.3° × 1.0°; x = 0.20, y = 0.35, 17.5 cd/m^2) that

appeared within a 11.1° × 8.3° region around fixation (**Figure 1**). For each display, the line coordinates were determined randomly, with restrictions that the lines did not overlap, that the left and right hemifields contained an equal number of lines, and that no line fell on the horizontal or vertical meridian. Singleton-absent displays contained 8, 12, or 16 lines of the same orientation (vertical or horizontal). Singleton-present displays were identical to singleton-absent displays except one of the lines was replaced with a line of an orthogonal orientation. The resulting 12 types of displays (set size x singleton presence x orientation) were intermixed randomly and presented with equal probability. Each display was presented for 750 ms, and the time between stimulus onset varied randomly between 1,350 ms and 1,650 ms. Participants were instructed to maintain eye fixation on the central cross and to indicate the presence or absence of the singleton (target) by pressing either the right or left shoulder button with one of their index fingers. The stimulus-response mapping was counterbalanced across participants. The entire experiment was comprised of 35 blocks of 48 trials (1,680 trials total; 280 singleton-present displays for each set size), with participant-controlled rest periods between blocks. Participants were given at least one block of trials as practice to learn the task.

Behavioural Analysis

Trials on which participants responded incorrectly, too quickly (response time, RT < 100 ms), or too slowly (RT > 1,350 ms) were excluded from the analysis. Mean RTs for target-absent and target-present trials at each set size were computed separately for each participant. A two-way, repeated-measures ANOVA was used to assess RTs as a function of set size (8, 12, 16) and singleton presence (present, absent). RTs from 8-item and 16-item displays were then compared using two-tailed, paired-sample *t* tests (separately for target-present and target-absent trials) to evaluate the effect of set size on RTs. Because of the inherent difficulty of asserting null hypotheses, we additionally computed the Bayes Factor (BF) for all nonsignificant statistical results. A default scale r (Cauchy scale) value of .707 was used to compute all BFs. We reported BF_{01} values to denote the likelihood of observing the data given the null hypothesis is true relative to observing the data given the alternative hypothesis is true.

Electrophysiological Recording and Analysis

EEG signals were recorded with 25 sintered Ag/AgCl electrodes housed in an elastic cap. The electrodes were positioned at standard 10-10 sites (FP1, FPz, FP2, F7, F3, Fz, F4, F8, T7, C3, Cz, C4, T8, P7, P3, Pz, P4, P8, PO7, POz, PO8, O1, Oz, O2, M1) and were referenced to an electrode positioned on the right mastoid during recording. The horizontal electrooculograph (HEOG) was recorded using two additional electrodes placed one centimeter from the external canthus of each eye and referenced to each other. The ground electrode was positioned over the midline frontal scalp at site AFz. The HEOG was used to detect eye movements away from the fixation cross. Eye blinks were monitored using an electrode above the left eye (at FP1). All electrode impedances were kept below 15 kΩ. EEG and EOG signals were amplified with a gain of 20,000, filtered using a bandpass filter of .01–100Hz (two-pole Butterworth), and digitized at 500 Hz. The EEG signals were stored on a computer for offline averaging. A semiautomated procedure was performed to remove epochs of EEG that were contaminated by horizontal eye movements, blinks, or amplifier blocking using our standard lab procedures (Tay et al., 2022). Artifact-free data were then low-pass filtered (half-power cutoff) at 30 Hz to create averaged ERP waveforms. Each EEG channel was digitally re-referenced to the average of the left and right mastoid channels. The grand-averaged event-related EOG deflections were required to be below 2 μV for further inclusion of the data in the analysis.

ERPs were computed from artifact-free epochs of EEG and HEOG signals, separately for singleton-present and singleton-absent displays. ERPs for singleton-present displays were further subdivided based on set size. For singleton-present displays, ERPs recorded contralateral and ipsilateral to the singleton were constructed using conventional methods (by collapsing across left- and right-field stimuli and left and right hemisphere electrodes). Two types of difference waves were computed to isolate the two ERP components of interest. First, ipsilateral ERPs were subtracted from corresponding contralateral ERPs (at each mirror-symmetric pair of lateral electrodes, such as PO7 and PO8) to isolate the N2pc. Second, target-absent ERPs were subtracted from target-present ERPs (separately for contralateral and ipsilateral waveforms) to isolate the SDP. Positive voltages were plotted downward by convention.

All ERP measurements were taken from waveforms recorded at PO7 and PO8, because visually evoked peaks (P1 and N1) and attention-related components (e.g., N2pc) are typically largest at or near these electrodes (Luck and Hillyard, 1994a, 1994b; Eimer, 1996; Hickey, Di Lollo, & McDonald, 2009) and because measurements were taken at these electrodes in previous studies of singleton detection (Tay et al., 2019, Tay et al., 2022). All N2pc measurements were performed on the contralateral-ipsilateral difference waves elicited by singletons in the lower visual field to maintain consistency with a prior study (Tay et al., 2019) and because the N2pc is larger for targets in the lower field than in the upper field (Luck, Girelli, McDermott, & Ford, 1997; Tay et al., 2019). All SDP measurements were performed on the ipsilateral present-absent difference waves elicited by singletons in both upper and lower visual fields to maintain consistency with prior studies (Tay et al., 2019; Tay et al., 2022) and because the magnitude and timing of the contralateral SDP would be obscured by the overlapping N2pc.

The latencies of the N2pc and SDP were measured as the time point at which the ERP deflection reached 50% of its peak amplitude. Differences in onset latencies (e.g., across different set sizes) were evaluated statistically using a conventional jackknife approach that replaces individual-subject data with N-1 sub-averages (and later correcting for the reduced variability; Miller, Patterson, & Ulrich, 1998; Kiesel, Miller, Jolicœur, & Brisson, 2008; Smulders, 2010). The mean-amplitude measurement window of the N2pc was defined as the 100-ms window following the point at which the N2pc in the grand-averaged contralateral-ipsilateral difference waveform first reached 50% of its peak amplitude (collapsed across set size). This measurement window turned out to be 192–292 ms (relative to stimulus onset). The magnitude of the SDP was quantified as the mean amplitude 200–400 ms post stimulus onset. These windows were selected a priori based on the typical durations of the components.

The presence of the N2pc was assessed separately for each set size using one-tailed, one-sample *t* tests (against zero microvolts). To test whether the N2pc becomes larger with increased set sizes, the mean amplitude of the lower-field N2pc was compared across the three set sizes using a one-way, repeated measures ANOVA followed by one-tailed, paired-sample *t* tests comparing amplitude of N2pc between 8- and 12-item displays and between 8- and 16-item

displays. The family-wise error rate was kept at .05 for each set of multiple comparisons using Bonferroni correction. The 50% fractional peak latency of the lower-field N2pc was then compared across the three set sizes using a one-way, repeated measures ANOVA (note: no follow-up comparisons were made because the ANOVA indicated no latency difference across the three set sizes). To determine whether the N2pc is larger or earlier on fast-response trials, one-tailed, paired-sample *t* tests were used to compare the amplitude and latency of N2pc obtained on fast- and slow-response trials (for lower-field singletons) using an RT-based median split to separate trials (McDonald et al., 2013). ERPs of fast- and slow-response trials were computed separately for each set size first then collapsed across the three set sizes.

Statistical analyses of the SDP were identical to those for the N2pc except for the following. In addition to the planned analysis of the 50% fractional peak latency (i.e., “onset” latency), we performed exploratory analyses using the 90% fractional peak latency to determine if set size and/or response speed influenced the “peak” timing of the SDP. To evaluate the effect of set size, a one-way, repeated measures ANOVA was performed and followed by two-tailed, paired-sample *t* tests comparing latency of SDP between 8- and 12-item displays and between 8- and 16-item displays. To evaluate the effect of fast and slow responses, a paired-sample *t* test was used to compare latency of SDP between fast- and slow-response trials (collapsed across set size). These exploratory analyses were based on the observation that although the SDP began at roughly the same time across set size, the time it takes to reach peak activity seemed to vary as a function of set size and speed of response.

Because the N2pc and SDP were found to increase with larger set sizes despite the absence of an RT effect (i.e., the slope of the RT set-size function was flat), an exploratory analysis was performed to determine whether the electrophysiological measures were more sensitive than the behavioural measures in revealing effects of set size on search efficiency. Participants were rank ordered based on differences in their RTs between set-size-16 trials and set-size-8 trials. A median split of this difference was then performed to separate participants who responded more quickly on set-size-16 trials than on set-size-8 trials (efficient-search group) from those who did not (inefficient-search group). The N2pc and SDP were then computed separately

for each group. Two-way, mixed ANOVAs were used to assess N2pc and SDP amplitude as a function of search efficiency (efficient-search group, inefficient-search group) and set size (8, 16). N2pc and SDP amplitudes elicited between two set sizes were then compared using two-tailed, paired-sample *t* tests for each group. If N2pc and/or SDP amplitudes are more sensitive to set size, then we would expect greater amplitude differences in the efficient-search group than in the inefficient-search group.

Topographical voltage maps of the ERP waveforms were constructed by spherical spline interpolation (Perrin, Pernier, Bertrand, & Echallier, 1989). All maps were created by collapsing over left and right targets and left and right electrodes such that electrodes on the left and right sides were ipsilateral and contralateral to the eliciting stimulus, respectively.

Results and Discussion

Approximately eight percent of trials were excluded from all analyses because responses were incorrect. Of the correct-response trials, 5.1% of were excluded because responses were too fast (RT < 100 ms) or too slow (RT > 1,350 ms). Lastly, 5.0% of the remaining trials were excluded because an artifact was detected in the electrophysiological recordings. RTs obtained from the remaining trials are presented in **Figure 2** as a function of set size and singleton presence. The two-way ANOVA revealed a significant Set Size main effect, $F(1.88, 184) = 19.30$, $p < .001$, $\eta^2_p = 0.27$, because the mean RTs were shorter for 16-item displays than for 8-item displays (i.e., a negative search slope). The Set Size x Singleton Presence interaction was also significant, $F(2, 196) = 7.04$, $p = .001$, $\eta^2_p = 0.13$, which indicates that the difference between RTs on 8- and 16-item trials was greater for singleton-absent trials than for singleton-present trials. There was no main effect of Singleton Presence, $F(1, 98) = 0.11$, $p = .737$, $BF_{01} = 0.89$. Planned comparisons revealed that RTs were statistically shorter for set size 16 than for set size 8 when the singleton was absent (554 ms vs. 566 ms, respectively), $t(49) = 6.18$, $p < .001$, $d = 0.87$, but not when the singleton was present (563 ms vs. 566 ms, respectively), $t(49) = 1.72$, $p = .092$, $BF_{01} = 1.66$. According to Bravo and Nakayama (1992), this flat search slope suggests that attention remained diffuse and no focal attention was involved in detection of the singleton.

Whether or not this is true, these behavioral results indicate that observers adopted a feature-free singleton detection strategy that enabled them to search efficiently.

---------- Insert Figure 2 about here ----------

Figure 3a displays the occipital ERP waveforms recorded contralaterally and ipsilaterally with respect to the singleton, separately for each set size. The waveforms contained the usual P1 and N1 components peaking at approximately 100 ms and 165 ms, respectively, after the onset of the search display. The contralateral and ipsilateral waveforms largely overlap until the peak of the N1, at which time the contralateral waveform becomes more negative than the ipsilateral. This difference was isolated by plotting the contralateral-ipsilateral difference waves, which consisted primarily of a negative peak within the time range of the N2pc (170–300 ms). Results of one-sample *t* tests revealed that the mean amplitudes of the N2pc deflections were statistically more negative than zero for all set sizes, *t*s(49) ≥ 4.39, *p*s < .001, *d*s ≥ 0.62. These results indicate that orientation singletons elicited the N2pc for each set size used in the present experiment. Thus, the findings of Experiment 1 replicate results from other recent studies and provide converging evidence that the N2pc is evident in singleton detection mode (Mazza et al., 2009a; Schubö et al., 2004; Tay et al., 2019; Tay et al., 2022).

To evaluate the effect of set size, the N2pc deflections elicited by lower-field singletons were measured and compared across the 8-, 12-, and 16-item displays (**Figure 3b**). The mean amplitude of the N2pc was found to vary across the three set sizes, $F(2, 98) = 3.27$, $p = .042$, $\eta^2_p = 0.06$. Planned pairwise comparisons revealed that the N2pc was smaller for 8-item displays (-0.90 μV/ms) than for 12-item displays (-1.25 μV/ms) and 16-item displays (-1.30 μV/ms), *t*s(49) ≥ 2.12, *p*s ≤ .017, *d*s ≥ 0.30. In contrast, the timing of the N2pc appeared to be unaffected by set size. In each case, the N2pc began at approximately 170 ms, peaked at approximately 270 ms, and terminated at approximately 325 ms. Consistent with this observation, the 50% fractional peak latency of the N2pc did not vary as a function of set size, $F(2, 98) = 1.17$, $p = .315$, $BF_{01} = 5.69$. Taken alone, these findings indicate that an increase in singleton salience increases the magnitude of the N2pc without affecting the speed with which observers can orient attention to the target singleton. However, the N2pc deflections in Experiment 1 were all considerably earlier

than in a prior singleton detection experiment that was largely identical except that the set size was fixed at eight items (Tay et al., 2019). In that study, the N2pc to lower-field targets was observed 250–350 ms and was preceded by a nominally separate N1pc. The unexpected difference in N2pc timing between this and Tay et al.'s study might be due to the intermixing of set sizes in the present study. The precise cause of this difference would have to be ascertained in future studies. To evaluate whether faster responses were associated with larger or earlier N2pc in singleton detection mode, we measured the N2pc of lower-field singletons separately for fast- and slow-response trials (**Figure 3c**). The N2pc was found to be larger on fast-response trials (-1.38 μV/ms) than on slow-response trials (-1.01 μV/ms), $t(49) = 3.54$, $p < .001$, $d = 0.50$. However, the 50% fractional peak latencies of N2pc did not differ statistically across fast-response trials (192 ms) and slow-response trials (207 ms), $t(49) = 0.31$, $p = .379$, $BF_{01} = 6.21$.

---------- Insert Figure 3 about here ----------

Figure 4a shows the occipital ERP waveforms elicited by singleton-present and singleton-absent displays, averaged across set size. As was seen in **Figure 4a**, the singleton-absent waveform is less positive than the singleton-present waveforms in the time range of the P3. This difference was isolated by subtracting the singleton-absent waveform from each of the contralateral and ipsilateral singleton-present waveforms, separately for each set size. **Figure 4b** shows the scalp topography of this difference in the 350–400-ms time range along with maps of the constituent singleton-present and singleton-absent ERPs in the same interval. The singleton-absent map contains a positive-voltage maximum over the midline parietal scalp, and the singleton-present map contains this parietal positivity along with greater positivity over the lateral occipital scalp regions. The maps of the present-absent differences reveals the isolated occipital positivity—that is, the SDP—over the contralateral and ipsilateral occipital scalp regions. **Figure 4c** shows the ipsilateral SDP components separately for each set size. As in a pair of recent studies, the SDP was generally evident 200–500 ms after the appearance of the search display. Results of one-sample *t* tests revealed that the mean amplitudes of the SDP components were statistically more positive than zero for all set sizes, $ts(49) \geq 10.30$, $ps < .001$, $ds \geq 1.46$. These

results indicate that orientation singletons elicited the SDP for each set size used in the present experiment.

To evaluate the potential effects of set size on neural activities associated with singleton detection, the SDP components were compared across the 8-, 12-, and 16-item displays. The mean amplitude of the SDP was found to vary as a function of set size, $F(2, 98) = 4.72$, $p = .011$, $\eta^2_p = 0.09$. Planned pairwise comparisons revealed that the SDP was smaller for 8-item displays (2.10 μV/ms) than for 16-item displays (2.50 μV/ms), $t(49) = 3.06$, $p = .002$, $d = 0.43$. The mean amplitudes of the SDP for 8- and 12-item displays (2.27 μV/ms) were not statistically different, $t(49) = 1.34$, $p = .094$, $BF_{01} = 1.56$. In contrast, 50% fractional peak latency of the SDP did not vary as a function of set size, $F(2, 98) = 1.42$, $p = .247$, $BF_{01} = 4.60$. However, the exploratory analysis revealed that 90% peak latency of the SDP did vary as a function of set size, $F(2, 98) = 3.44$, $p = .034$, $\eta^2_p = 0.07$. Subsequent pairwise comparisons revealed that the SDP peaked later for 8-item displays (341 ms) than for 16-item displays (314 ms), $t(49) = 2.17$, $p = .035$, $d = 0.31$. The 90% fractional peak latencies of the SDP for 8- and 12-item displays (329 ms) were not statistically different, $t(49) = 1.26$, $p = .214$, $BF_{01} = 3.09$. These results indicate that an increase in singleton salience increases the magnitude of the SDP. In terms of SDP timing, an increase in singleton salience appears to not affect the onset of SDP but possibly increases the speed at which it reaches maximal activity.

To determine whether the characteristics of the SDP is associated with overt performance, we computed the mean amplitude and 50% fractional peak latency of the SDP separately for fast- and slow-response trials (**Figure 4d**). The SDP was found to be larger on fast-response trials (2.78 μV/ms) than on slow-response trials (1.94 μV/ms), $t(49) = 5.58$, $p < .001$, $d = 0.79$, but the planned analysis of latency revealed no significant difference between fast-response trials (259 ms) and slow-response trials (270 ms), $t(49) = 1.46$, $p = .075$, $BF_{01} = 2.41$. However, the exploratory analysis based on 90% fractional peak latency of the SDP revealed that the SDP peaked earlier on fast-response trials (312 ms) than on slow-response trials (345 ms), $t(49) = 3.41$, $p = .001$, $d = 0.48$. These results provide additional evidence that the SDP reflects a process involved in the detection of a target singleton. Specifically, efficient detection

performance was associated with larger and earlier-peaking SDP activities at the level of the individual participant.

Although there was no statistical difference between singleton-present RTs of 8- and 16-item displays, we nevertheless found the amplitudes of the N2pc and SDP to increase with larger set sizes. This mismatch suggests that the ERP measures are more sensitive than the behavioral measures to variations in attentional processes. To evaluate this possibility, we sorted participants into two groups (efficient-search group vs. inefficient search group) based on a median split of RT difference between 8- and 16-item displays that contained a singleton. A two-way, mixed ANOVA test of N2pc amplitude revealed a main effect of set size, $F(1, 48) = 5.22$, $p = .027$, $\eta^2_p = 0.10$ and an interaction of set size and search efficiency, $F(1, 48) = 5.67$, $p = .021$, $\eta^2_p = 0.11$. Paired *t* tests revealed that while there was no difference in N2pc amplitude across 8- (-0.83 μV/ms) and 16-item (-0.81 μV/ms) displays for the inefficient-search group, $t(24) = 0.06$, $p = .950$, $BF_{01} = 4.73$, the N2pc was larger on 16- (-1.80 μV/ms) than 8-item (-0.97 μV/ms) displays for the efficient-search group, $t(24) = 3.62$, $p = .001$, $d = 0.72$ (**Figure 3d**). A similar ANOVA on SDP amplitudes revealed a main effect of set size, $F(1, 48) = 9.19$, $p = .004$, $\eta^2_p = 0.16$, but no significant interaction between set size and search efficiency, $F(1, 48) = 0.12$, $p = .726$, $BF_{01} = 3.52$. These results indicate that the increase in N2pc amplitude with larger set sizes is associated with increase in search efficiency and that N2pc amplitude is a more sensitive measure of search efficiency than RT.

---------- Insert Figure 4 about here ----------

Experiment 2

Experiment 1 examined the effects of set size on the ERP componentry of singleton detection mode and provided evidence for the target processing hypothesis of the N2pc as well as the role of SDP in singleton detection. However, little is known about the possible neural sources of the SDP or the singleton-detection N2pc. Assuming that the singleton-detection N2pc arises from the same selective processes as in feature-guided search, the singleton-detection N2pc should, in principle, arise from some region of extrastriate visual cortex. In one seminal report, the scalp

topography of the N2pc was isolated over the contralateral scalp by subtracting ERPs elicited by easy-to-ignore nontarget singletons from ERPs elicited by attended target singletons (Luck & Hillyard, 1994a). In a later study (Hopf et al., 2000), the topography of the N2pc and its magnetic equivalent (the mN2pc) were shown by subtracting right-target ERPs from left-target ERPs (using identical displays that contained a target on one side and a nontarget singleton on the other). Such a subtraction produces a negativity on the right side of the scalp and a positivity on the left side of the scalp, which are considered to reflect N2pc to left- and right-field targets, respectively (the positivity is an N2pc to right-field targets, which is inverted in polarity due to the subtraction procedure). Using such data, the N2pc was estimated to arise from a source in the inferior temporal gyrus of the contralateral visual cortex (Hopf et al., 2000). Three caveats must be considered, however. First, the source estimates were based on the mN2pc and then used to account for the N2pc. Second, although the method of isolating N2pc successfully removes purely sensory activities, it combines left-target N2pc with an inverted right-target N2pc into one complex scalp distribution. In doing so, this method makes it impossible to visualize activities over the ipsilateral scalp (since those activities are presumed to be associated with the contralateral target). Third, because a target singleton must be accompanied by a nontarget singleton on the other side of fixation, some of the observed difference-wave activity may be related to active suppression of the nontarget singleton rather than selection of the target singleton (Hickey et al., 2009; Gaspar & McDonald, 2014). Accordingly, one goal of Experiment 2 was to estimate the neural sources of the N2pc using a different isolation procedure. However, the primary goal of Experiment 2 was to better characterize the scalp topography and investigate the potential neural sources of the SDP, since there is little information about the potential sources of this recently discovered ERP component.

Materials and Methods

Participants

The methods for recruitment and screening of participant were identical to those in Experiment 1. Sixteen students participated after giving informed consent. Data from two participants were excluded from further analyses due to excessive artifacts. Of the remaining 14

participants (mean age: 20.6 years), 12 were female and 13 were right-handed. The sample size of the present experiment was predetermined to have sufficient power (.80) to detect moderately large ERP effects (d = 0.70) because we expected 16-item displays to elicit, at minimum, moderately large N2pc and SDP components.

Apparatus

The apparatus in Experiment 2 was identical to those in Experiment 1 except visual stimuli were presented on a 19-inch CRT monitor from a distance of 100 cm.

Stimuli and Procedure

The stimuli and procedure in Experiment 2 were identical to those in Experiment 1 except every display contained 16 grey lines (RGB: 174, 174, 174) within a 9.0° × 9.0° region around fixation. The entire experiment was comprised of 10 blocks of 80 trials.

Electrophysiological Recording and Analysis

EEG was recorded using 63 tin electrodes referenced to a tin electrode on the right mastoid. Most electrodes were positioned at standard 10-10 sites, but five electrodes were positioned at nonstandard sites that were inferior to the standard occipital electrodes to better characterize the topography of visual evoked activities over the posterior scalp. HEOG was recorded from a pair of tin electrodes. All other aspects of recording, EEG pre-processing were identical to those in Experiment 1. N2pc and SDP were measured for all singletons regardless of whether they were in the upper or lower field. Presence of the N2pc and SDP were assessed using one-tailed, one-sample t tests against zero microvolts.

Following analysis of the scalp-recorded ERPs, the grand-averaged present-absent difference waves were exported to BESA software (version 6.1) in order to estimate the loci of discrete neural sources of the N2pc and SDP. The subtraction procedure used to create these difference waves removes all activities that are common to the singleton-present and singleton-absent displays, including the P1, N1, and P3b components (Tay et al., 2019; Tay et al., 2022). Unlike other methods used to isolate the N2pc (e.g., left-minus-right), this subtraction procedure does not amalgamate activities associated with multiple targets and concurrent distractors. The

resulting difference waves are dominated primarily by the SDP and overlapping N2pc over the posterior scalp.

A four-shell ellipsoidal model was used to represent the conductivities of the brain, cerebral-spinal fluid, skull, and scalp. To model the neural sources of the larger SDP, a pair of mirror-symmetric regional sources were fit in a 100-ms time window that began after the time period of the N2pc (300–400 ms). The BESA algorithm alters the locations, orientations, and strengths of the two regional sources until the modeled scalp topography (i.e., forward solution) provides the best fit to the data. After the best two-source fit was found, a principal component analysis (PCA) of the residual waveforms (i.e., unmodelled activities) was performed to determine whether an additional source should be added to the model. A two-source model was deemed sufficient to account for the SDP because (1) there was no clear PCA component in the residual data, and (2) a source added to account for the residual noise ended up outside of the coordinates of the brain. The coordinates of the best-fitting regional sources were estimated in BESA and were related to known anatomy using an online brain atlas (the MNI <-> Talaraich Tool; BioImage Suite Web).

Source analysis of the N2pc was performed in a similar way, but the difference waves were first high-pass filtered (in BESA) using a pair of Butterworth digital filters (forward and backward to prevent phase shifting). This combined, zero-phase filter had a half-amplitude cutoff at 2 Hz and a slope of 12 dB/octave. This filter was applied to attenuate the lower-frequency SDP, thereby enabling the N2pc to appear as a negativity rather than a negative-going voltage superimposed on a larger positivity. After filtering, a pair of mirror-symmetric regional sources were fit in a 170–262-ms window that included the early phase of the N2pc but avoided overlap with the residual SDP at longer latencies. As with the SDP source analysis, no additional source was deemed necessary to account for the N2pc within the fit interval.

Results and Discussion

Less than nine percent of the trials were excluded from analyses because responses were incorrect, too fast (RT < 100 ms), or too slow (RT > 1,350 ms). Of the remaining trials, 13.3% were further excluded because an artifact was detected in the EEG recordings. Mean RTs from the remaining singleton-present and singleton-absent trials were 535 ms and 533 ms,

respectively. The 2-ms difference between the mean RTs was not significant, $t(13) = 0.28$, $p = .785$, $BF_{01} = 3.58$.

As in Experiment 1, the N2pc and SDP were evident in the ERPs recorded over the lateral posterior scalp (**Figures 5a and 5b**). One-sample *t* tests confirmed the presence of the SDP (1.99 μV/ms), $t(13) = 7.40$, $p < .001$, $d = 1.98$, and the presence of the N2pc (-1.31 μV/ms), $t(13) = 7.98$, $p < .001$, $d = 2.13$. The 50% fractional peak latencies of the SDP and the N2pc were 244 ms and 206 ms, respectively, which is similar to the latencies of the SDP (258 ms) and N2pc (203 ms) elicited by 16-item displays in Experiment 1.

Figure 5c displays the scalp topography of the present-absent waveforms using the 64-channel electrode array employed in Experiment 2. As in Experiment 1, the SDP was evident bilaterally over the posterior scalp. Early on (200–300 ms post stimulus), the temporally and spatially overlapping N2pc countered the positive maximum over the contralateral scalp (right side of heads), but this lateralization eventually reversed as the contralateral difference waveform became slightly more positive than the ipsilateral waveform. This post-N2pc positivity has been labelled the target P_D (Sawaki, Geng, & Luck, 2012) or target positivity (P_T; Jannati, Gaspar, & McDonald, 2013).

To estimate the neural sources of the SDP, grand-averaged present-absent difference waves were exported to BESA. Because the topography showed an increase in bilateral occipital positivity over time without any apparent rotation of the voltage distribution, we modeled the neural generators of the SDP using a pair of mirror-symmetric regional sources. The forward solution of the best-fitting two-source model closely resembled the observed scalp topography of the SDP (**Figure 6a**). This regional-source model accounted for 98.13% of the variability in the present-absent difference waves in the 300–400-ms SDP fit interval. The coordinates of the best-fitting regional sources fell within the ventral extrastriate cortex (Talairach coordinates: $x = \pm 28.8$, $y = -76.8$, $z = -9.5$; **Figure 6b**).

The scalp topography of the N2pc is more difficult to visualize because that component is superimposed upon the larger SDP over the posterior scalp (see **Figures 5b** and **5c**). To visualize the N2pc topography, prior studies plotted maps of the left-right difference waveforms

(e.g., Girelli & Luck, 1997; Hopf et al., 2000) or the contralateral-ipsilateral difference waveforms over one side of the scalp (e.g., Hickey et al., 2009) or over the entire scalp (for whole-head mapping of the contra-ipsi difference waves, the difference has to be plotted at both contralateral and ipsilateral electrodes; e.g., Kiss, Van Velzen, & Eimer, 2008). **Figure 5d** shows the topography of the current N2pc data using each of these two approaches. As noted in the introduction to Experiment 2, the left-right difference map combines a left-target N2pc and an inverted right-target N2pc into one map. The symmetric map of the contra-ipsilateral difference wave avoids this complication but introduces other problems by duplicating the difference across both sides of the scalp. In particular, because there is no contralateral-ipsilateral difference along the midline of the scalp (running from nasion to inion), the duplicate N2pc maxima may be misplaced too far laterally. In addition, both mapping approaches assume N2pc to be driven entirely by contralateral activity and are essentially blind to activities over the ipsilateral hemisphere. These scalp-level problems continue to exist in so-called source space when the goal is to estimate where the neural sources of the N2pc (or other lateralized ERP components) are located. One study estimated that the conventional topographical mapping approaches can lead to errors in source localization of up to 40% (Oostenveld et al., 2003).

Because of these potential problems, we did not attempt to analyze the sources of the left-right difference waveforms or the mirror-symmetric map of the contralateral-ipsilateral difference waveforms shown in **Figure 5d**. Instead, we simply applied a high-pass filter (2-Hz cutoff) to the present-absent difference waveforms in order to attenuate the lower-frequency SDP while preserving the N2pc. **Figure 6c** illustrates the results of this high-pass filtering. The filtered SDP is attenuated compared to the original SDP (**Figure 5b**), thereby making the N2pc appear as a contralateral negativity rather than a negative-going voltage superimposed on a larger positivity. **Figure 6d** shows a current source density (CSD) map of the N2pc following this additional filtering step. The CSD map shows a clear radial current source over the contralateral scalp (right side of head) without a duplicate source over the ipsilateral scalp (which would necessarily occur for left-right difference maps and symmetric contra-ipsi maps). The neural generators of this N2pc was modelled using a pair of mirror-symmetric regional sources. The forward solution of the best-

fitting model closely resembled the observed scalp topography of the N2pc (**Figure 6d**). The model accounted for 96.24% of variability in the 170–262-ms N2pc fit interval. The coordinates of the best-fitting regional sources fell within the ventral extrastriate cortex (Talairach coordinates: x = ± 28.3, y = -79.2, z = -7.8; **Figure 6e**), in the vicinity of the estimated mN2pc dipolar source within the left fusiform gyrus (Hopf et al., 2000).

General Discussion

The twin aims of the present study were to determine how salience (as manipulated by set size) affects the ERP signatures of singleton detection mode and to estimate the neural sources of these ERP signatures. In addition, the results have implications for the long-standing issue about the involvement of attention in the detection of simple visual features and about the selection processes that have been hypothesized to give rise to the N2pc and SDP.

Salience modulates N2pc and SDP but not grand-averaged RTs

In Experiment 1, we showed that the grand-averaged RTs on singleton-present trials did not vary as a function of set size. Consistent with this behavioural result, we found that the onset latencies of the N2pc and SDP (as defined by their 50% fractional peak) did not vary as a function of set size nor as a result of RT-based median split. Interestingly, the N2pc onset latency was shorter here than in a previous study that used a fixed set size of eight items (Tay et al., 2019) and was more in line with a recent study that used a fixed set size of 16 items (Tay et al., 2022, Experiment 2, figure 6b). The reason for the timing discrepancy is unclear, but it might be a consequence of intermixing trials of different set sizes. Further experimentation will be needed to ascertain the precise cause of this unexpected difference.

Contrary to what one might expect from a flat search slope, we observed changes in amplitudes of the N2pc and SDP across the three set sizes. Specifically, N2pc and SDP were larger for 12- and 16-item displays than for 8-item displays. Thus, there was a mismatch between set-size effects on the ERP signatures of singleton detection and on the conventional behavioural performance measures. A different mismatch was observed in a previous study of feature search mode (Christie, Livingstone, & McDonald, 2015). There, observers searched for one of two

prespecified colours in displays containing four, six, eight, or ten different-coloured rings. RTs were found to increase with set size (a slope of ~15 ms/item), but neither the amplitude nor onset latency of the target-elicited N2pc varied as a function of set size. This finding and the current finding together demonstrate that behavioural search slopes do not provide definitive information about search efficiency. Indeed, RTs represent the summed output of multiple processes, some of which (e.g., later processes associated with response selection) might be negatively affected by set size.

The mismatch between behavioural and electrophysiological measures of attention suggests that the conventional behavioural measures are not as sensitive as the isolated ERP signatures of attentional selection. To help test this sensitivity explanation and to move away from a strict reliance on grand-averaged measures of performance, we sorted participants into two groups based on a median split of RT difference between set-size-8 trials and set-size-16 trials. Participants in the efficient-search group detected the target faster on 16-item-display trials than on 8-item-display trials (i.e., displayed a negative search slope), while participants in the inefficient-search group showed the reverse effect or no difference. On the assumption that a negative search slope indicates the involvement of focused attention in visual search (Bravo & Nakayama, 1992), we surmised that the amplitude of the N2pc would vary more as a function of set size for the efficient-search group than for the inefficient-search group. This was exactly what was found. This exploratory finding indicates that (1) grand-averaged N2pc amplitude is a more sensitive index of focused attention than is grand-averaged RT and (2) individual differences in RT search slopes are associated with individual differences in ERP measures of attentional selection.

A similar link between N2pc and RT was observed by Drisdelle, West, and Jolicœur (2016) in a feature-based, target-discrimination task. In that study, the authors performed RT-based median splits that first divided participants into fast- and slow-responder groups and then subdivided trials within each group into fast- and slow-response trials. They found the N2pc to be smallest and to occur latest for slow-response trials among slow responders and to be largest and earliest for fast-response trials among fast responders. The combined results of Drisdelle et

609 al.'s study and the present study suggest that selective attention operates similarly regardless of
610 the search mode adopted.
611 Here we note two interesting post-hoc observations from Experiment 1. First, although onset
612 latency of the SDP did not vary with set size, the time at which it reached its peak (as defined by
613 its 90% fractional peak) was earlier with increased set size. Second, the SDP did not appear to
614 begin before the N2pc, as it did in previous studies (cf. Tay et al., 2019; Tay et al., 2022),
615 indicating that the SDP does not reflect detection processes that must precede attentional
616 selection. These observations suggest that the SDP is more closely associated with processes
617 involved in the conscious awareness of a target singleton rather than the preattentive detection
618 mechanism itself. This view would be consistent with the observation that the SDP always
619 reaches peak activity following N2pc offset (**Figure 5b**; Tay et al., 2019; Tay et al., 2022),
620 presumably because attentional selection of a singleton would lead to greater awareness of its
621 presence. Alternatively, the SDP and N2pc might simply reflect separate selection mechanisms
622 with different time courses under different conditions, since only the latter component is
623 associated with search efficiency under the present experimental condition.

624 **Attentional involvement in the detection of visual singletons**

625 There has been a long debate about whether the detection of simple visual features or
626 feature differences, such as colour or orientation, requires attention. According to feature
627 integration theory, detection of a known feature can be achieved without focal attention or spatial
628 selection by monitoring activity within a relevant feature map directly (Treisman, 1985; Treisman
629 & Gormican, 1988). Search for such features has been characterized as being accomplished
630 preattentively or in parallel to contrast it with more challenging search tasks that require focal
631 attention. This characterization has been based on behavioural performance measures, such as
632 RTs, that remain unchanged as more items are added to the search display. According to Bravo
633 and Nakayama (1992), detection can be accomplished without focal attention when the target is
634 known (consistent feature mapping) or unknown (variable feature mapping). Other researchers
635 have hypothesized that attentional selection is required for detection as well as for discrimination
636 (e.g., Theeuwes, 2010). In line with this latter perspective, visual detection is impaired

637 immediately after another attentionally demanding task was performed (Joseph, Chun, &
638 Nakayama, 1997).
639 On the assumption that the N2pc reflects an early stage of attentional selection (Luck, 2012;
640 Luck & Hillyard, 1994b; Eimer & Kiss, 2010), ERPs recorded in visual-search tasks demonstrate
641 that detection of simple features typically involves attention. This appears to be the case with
642 consistent mapping of target and nontarget features (e.g., Luck & Hillyard, 1994a, 1994b) and
643 with variable mapping procedures that preclude the use of a feature search mode (present
644 experiment; see also, Mazza et al., 2009a; Schubö et al., 2004; Tay et al., 2019; Tay et al., 2022).
645 The presence of N2pc in such detection tasks does not indicate definitively that attentional
646 selection is necessary for detection, as posited by some theoretical perspectives (e.g.,
647 Theeuwes, 2010), but it does demonstrate that attentional selection occurs when there is no effort
648 to prevent such selection. There is some indication that detection can take place in the absence
649 of an N2pc, at least under consistent-mapping conditions. Specifically, Luck and Ford (1998)
650 found that the N2pc was eliminated when participants had to determine whether a letter
651 appearing at fixation was a consonant or vowel. A similar experiment will be needed in the future
652 to determine whether singleton detection can occur under variable-mapping conditions in the
653 absence of the N2pc.
654 The present findings and conclusions are slightly at odds with those of Bravo and
655 Nakayama's (1992) study. Briefly, those authors reported that under variable-mapping conditions,
656 RTs are unaffected by set size in a detection task (as was the case here) but became shorter with
657 increasing set size in a compound-search task. The negative search slope was taken as evidence
658 for the involvement of focused attention in visual-discrimination tasks, and the flat search slope
659 was taken as evidence for the involvement of distributed attention in visual-detection tasks. The
660 present ERP results, and those of prior variable-mapping detection studies (e.g., Mazza &
661 Caramazza, 2011; Mazza et al., 2009a), suggest that this distinction between focused attention
662 and distributed attention is not entirely correct, because attentional selection, as indexed by the
663 N2pc, was evident in singleton detection mode with no requirement for close scrutiny of the
664 singleton's features. From an electrophysiological perspective, the key difference between the

detection and discrimination tasks appears to be the presence and/or magnitude of a sustained posterior contralateral negativity (SPCN; Jolicœur et al., 2008) that sometimes appears following N2pc offset rather than the N2pc itself. Although the SPCN has been associated with visuospatial working memory and other "post-selection" processes (e.g., Jolicoeur et al., 2008; Vogel & Machizawa, 2004), it may be more appropriate to consider the N2pc and SPCN as indices of different stages of attentive processing (e.g., Jannati et al., 2013) and the entire duration of these components as index of the duration of attentive processing (i.e., the *attentional dwell time*; Duncan, Ward, & Shapiro, 1994). From this perspective, Bravo and Nakayama's negative search slope would be predicted whenever the attentive processing stage involves the selective processes reflected by the SPCN but should be absent when little to no such selective processing follows the N2pc.

Spatial filtering and the N2pc

Although there is general agreement that the N2pc is associated with the initial attentional selection of the eliciting stimulus, the specific neural process hypothesized to drive the N2pc has been debated for over two decades. Two main perspectives have emerged. According to the *filtering hypothesi*s, the N2pc reflects the attenuation of neural activity driven by nontarget items, not the enhancement of the attended item itself (Luck, 2012; Luck et al., 1997; note that Luck and Hillyard, 1994b, were more agnostic about whether filtering is accomplished by suppressing nontargets or enhancing the target). This attenuation is hypothesized to help resolve neural ambiguities that arise when multiple items fall within the same large receptive fields of neurons in extrastriate visual cortex. In contrast, according to the *target processing hypothesis*, the N2pc reflects the selective processing of the attended item itself (Eimer, 1996; Hickey et al., 2009; Mazza et al., 2009a, 2009b; Wijers, Lange, Mulder, & Mulder, 1997; Zivony, Allon, Luria, & Lamy, 2018). By this view, the N2pc might be involved in target enhancement (Zivony et al. 2018), feature analysis (Mazza et al., 2009a, 2009b), or object individuation (Mazza & Caramazza, 2015).

Luck and Hillyard's (1994b) seminal singleton-detection experiment was designed to test the filtering hypothesis. Those authors surmised that the variable-mapping of target and nontarget

orientations would prevent participants from using a filtering strategy to find the singleton target. Because the N2pc was not evident in their singleton-detection experiment, they concluded that the N2pc reflects a filtering mechanism that suppresses items in the vicinity of the attended object. However, a handful of subsequent studies did report finding the N2pc under variable-mapping conditions (Mazza et al., 2009a; Schubö et al., 2004; Tay et al., 2019; Tay et al., 2022). To account for such observations, Luck (2012) proposed that the filtering operation might be initiated automatically when the singleton is sufficiently salient, even though filtering would actually impair detection performance under variable-mapping conditions. Two of our present findings are at odds with this post-hoc *costly filtering* explanation. First, if filtering occurs more frequently with more salient singletons, we would expect RTs to increase with larger set sizes. However, the finding of a flat RT search slope here and in prior studies (e.g., Bravo & Nakayama, 1992) indicates that increased salience does not interfere with singleton detection. Second, if the N2pc reflects filtering, we would expect N2pc amplitude to be negatively associated with performance. In direct contrast to this expectation, the N2pc was found to be larger on fast-response trials than on slow-response trials.

Despite our evidence against the filtering hypothesis, suppressive filtering might still be an essential process involved in attentional selection. For example, the selective tuning model of visual attention (Tsotsos et al., 1995) posits that attentional selection involves tuning of activity throughout the hierarchical visual system via iterative exchanges between higher and lower levels in the system. The model instantiates this tuning process with a suppressive mechanism that "prunes" competing activations of nearby neurons at each layer of the visual hierarchy. By this view, the feed-forward sweep initiated by a multi-item visual display triggers a winner-take-all process at the top level of the system, centered on the unit that most likely represents the target (based on bottom-up activations and top-down expectations). This initial activation of the top level is hypothesized to be sufficient for detection of simple features but insufficient to discern details that require higher spatial resolution. In these latter situations, the winner-take-all process initiates feedback activity in the lower levels that suppress activations associated with stimuli at nearby, irrelevant locations. Previous MEG studies have uncovered evidence of an inhibitory zone

721 surrounding the attended item that is hypothesized to enable this selective-tuning process
722 (Boehler, Tsotsos, Schoenfeld, Heinze, & Hopf, 2011; Hopf et al., 2006; Hopf, Boehler,
723 Schoenfeld, Heinze, & Tsotsos, 2010), but the mN2pc was found to be independent of this
724 inhibitory surround (Boehler et al., 2011).

725 What other process might the N2pc and its magnetic equivalent represent if it does not reflect
726 suppressive filtering? One possibility is that it reflects the initial winner-take-all activity at the top
727 level, which leads to the detection of features (or singletons) or to further selective tuning when
728 necessary. On this hypothesis, the SPCN, rather than the N2pc, might be associated with
729 selective tuning. Note, however, that the N2pc might represent an early process associated with
730 target selection even in the absence of inhibitory-based selective tuning (Mazza & Caramazza,
731 2015; Wyble et al., 2020). Finally, although the N2pc appears to be associated with target
732 processing, attended targets may elicit the N2pc only when there is competition from at least one
733 other item in the display (Luck & Hillyard, 1994b; McDonald, Tay, Prime, & Hillyard, 2022). This
734 indicates that a competition-based, winner-take-all process is required for the elicitation of N2pc,
735 even if that process is resolved without inhibitory selective tuning.

736 **Singleton-detection processes in the human brain**

737 The present study identified the N2pc and SDP as ERP signatures of singleton detection.
738 The N2pc has been a well-documented electrophysiological marker of attention for nearly three
739 decades. This ERP component is observed whenever a singleton is attended under consistent-
740 mapping conditions (e.g., Luck & Hillyard, 1994b; Schubö & Müller, 2009) and, as shown here
741 and elsewhere, variable-mapping conditions (Mazza et al., 2009a, 2009b; Schubö et al., 2004;
742 Tay et al., 2019; Tay et al., 2022). Furthermore, prior studies have shown that the N2pc increases
743 in size with increased attentional focus (e.g., Luck et al., 1997), tracks serial shifts of attention
744 when observers must closely inspect multiple singletons to find a specific target (e.g., Woodman
745 & Luck, 1999), appears earlier for attended objects that were more salient (e.g., Gaspar &
746 McDonald, 2014), and is earlier when the visual system is primed for a repeatedly attended
747 feature across consecutive trials (e.g., Christie et al., 2015; Eimer, Kiss, & Cheung, 2010). The

present source analysis results indicate that the N2pc, like its magnetic counterpart (mN2pc), is generated in the ventral stream of visual cortex.

By comparison, much less is known about the SDP. This ERP component differs from the well-known P3b in two ways. First, the SDP is associated with singleton-present displays, whereas the P3b is elicited by both singleton-present and singleton-absent displays. Second, the SDP is maximal bilaterally over the occipital scalp, whereas the P3b is maximal over the midline parietal scalp. The high-density mapping of SDP in Experiment 2 confirmed the occipital SDP maxima and showed that it reflects radial source activities over lateral occipital scalp regions. Consistent with these scalp-level observations, the results of our source analysis indicate that the SDP likely arises from neural sources in ventral extrastriate visual areas of the occipital lobes. By contrast, the generator of the P3b has been localized to areas of the parietal and inferior temporal lobes (e.g., Bledowski et al., 2004).

Although the SDP has been isolated in singleton-detection tasks involving variable-feature mapping, the processes giving rise to the SDP might not be specific to such conditions or to singleton detection mode. Indeed, SDP-like activities have been reported in at least a couple of studies involving consistent-mapping procedure (although these activities were nominally associated with the P3; Luck and Hillyard, 1990, 1994a). For example, Luck and Hillyard (1990) concluded that the occipital P3 may reflect processes underlying the detection of targets defined by the presence of a fixed, unique feature and that this process occurs prior to the identification of complex objects. Here we offer two possible explanations as to why the SDP may be observable under consistent-mapping conditions. First, the SDP (like the N2pc) could arise when a simple visual feature is detected, regardless of search strategy. Second, when both search modes are possible (as in a consistent-mapping procedure), observers might opt for singleton detection mode by default (Bacon & Egeth, 1994; Leber & Egeth, 2006).

The SDP might also be related to bilateral occipital gamma-band activity triggered by line segments that are configured into consciously perceived shapes (Pitts, Padwal, Fennelly, Martínez, & Hillyard, 2014). The shape appeared against a background of randomly oriented line segments, so like the variable-mapping singleton detection task, this task would have prompted

776 comparisons of adjacent items with no need for filtering. Given the similarities, it is possible the
777 SDP and gamma-band activity might reflect similar processes in bilateral visual cortices.
778

References

Bacon, W. F., & Egeth, H. E. (1994). Overriding stimulus-driven attentional capture. *Perception & Psychophysics*, *55*, 485–496. https://doi.org/10.3758/BF03205306

Bledowski, C., Prvulovic, D., Hoechstetter, K., Scherg, M., Wibral, M., Goebel, R., & Linden, D. E. (2004). Localizing P300 generators in visual target and distractor processing: a combined event-related potential and functional magnetic resonance imaging study. *Journal of Neuroscience*, *24*(42), 9353–9360. https://doi.org/10.1523/JNEUROSCI.1897-04.2004

Boehler, C. N., Tsotsos, J. K., Schoenfeld, M. A., Heinze, H. J., & Hopf, J. M. (2011). Neural mechanisms of surround attenuation and distractor competition in visual search. *Journal of Neuroscience*, *31*(14), 5213–5224. https://doi.org/10.1523/JNEUROSCI.6406-10.2011

Bravo, M. J., & Nakayama, K. (1992). The role of attention in different visual-search tasks. *Perception & Psychophysics*, *51*, 465–472. https://doi.org/10.3758/BF03211642

Bundesen, C. (1990). A theory of visual attention. *Psychological Review*, *97*, 523–547.

Burra, N., & Kerzel, D. (2013). Attentional capture during visual search is attenuated by target predictability: Evidence from the N2pc, Pd, and topographic segmentation. Psychophysiology, 50(5), 422–430.

Carlisle, N. B., Arita, J. T., Pardo, D., & Woodman, G. F. (2011). Attentional templates in visual working memory. *Journal of Neuroscience*, *31*, 9315–9322. https://doi.org/10.1523/JNEUROSCI.1097-11.2011

Chelazzi, L., Duncan, J., Miller, E. K., & Desimone, R. (1998). Responses of neurons in inferior temporal cortex during memory-guided visual search. *Journal of Neurophysiology*, *80*, 2918–2940. https://doi.org/10.1152/jn.1998.80.6.2918

Chelazzi, L., Miller, E. K., Duncan, J., & Desimone, R. (1993). A neural basis for visual search in inferior temporal cortex. *Nature*, *363*, 345–347. https://doi.org/10.1038/363345a0

Christie, G. J., Livingstone, A. C., & McDonald, J. J. (2015). Searching for inefficiency in visual search. *Journal of Cognitive Neuroscience*, *27*(1), 46–56. https://doi.org/10.1162/jocn_a_00716

Desimone, R., & Duncan, J. (1995). Neural mechanisms of selective visual attention. *Annual Review of Neuroscience*, *18*, 193–222. https://doi.org/10.1146/annurev.ne.18.030195.001205

Dowdall, J. R., Luczak, A., & Tata, M. S. (2012). Temporal variability of the N2pc during efficient and inefficient visual search. *Neuropsychologia*, *50*, 2442–2453. https://doi.org/10.1016/j.neuropsychologia.2012.06.015

Drisdelle, B. L., West, G. L., & Jolicoeur, P. (2016). The deployment of visual spatial attention during visual search predicts response time: electrophysiological evidence from the N2pc. Neuroreport, 27(16), 1237–1242. https://doi.org/10.1097/WNR.0000000000000684

Duncan, J. (1985). Visual search and visual attention. In M. I. Posner & O. S. M. Marin (Eds.), *Attention and performance XI* (pp. 85–106). Hillsdale, NJ: Erlbaum.

Duncan, J., & Humphreys, G. W. (1989). Visual search and stimulus similarity. *Psychological Review*, *96*, 433–458. https://doi.org/10.1037/0033-295X.96.3.433

Duncan, J., Ward, R., & Shapiro, K. (1994). Direct measurement of attentional dwell time in human vision. *Nature*, *369*(6478), 313–315. https://doi.org/10.1038/369313a0

Eimer, M. (1996). The N2pc component as an indicator of attentional selectivity. *Electroencephalography and Clinical Neurophysiology*, *99*, 225–234. https://doi.org/10.1016/0013-4694(96)95711-9

Eimer, M., Kiss, M., & Cheung, T. (2010). Priming of pop-out modulates attentional target selection in visual search: Behavioural and electrophysiological evidence. *Vision Research*, *50*(14), 1353–1361. https://doi.org/10.1016/j.visres.2009.11.001

Folk, C. L., Remington, R. W., & Johnston, J. C. (1992). Involuntary covert orienting is contingent on attentional control settings. *Journal of Experimental Psychology: Human Perception and Performance*, *18*, 1030–1044. https://doi.org/10.1037/0096-1523.18.4.1030

Gaspar, J. M., & McDonald, J. J. (2014). Suppression of salient objects prevents distraction in visual search. *Journal of Neuroscience*, *34*, 5658–5666. https://doi.org/10.1523/JNEUROSCI.4161-13.2014

Girelli, M., & Luck, S. J. (1997). Are the same attentional mechanisms used to detect visual search targets defined by color, orientation, and motion? *Journal of Cognitive Neuroscience*, *9*(2), 238–253. https://doi.org/10.1162/jocn.1997.9.2.238

Hickey, C., McDonald, J. J., & Theeuwes, J. (2006). Electrophysiological evidence of the capture of visual attention. *Journal of Cognitive Neuroscience*, *18*(4), 604–613. https://doi.org/10.1162/jocn.2006.18.4.604

Hickey, C., Olivers, C., Meeter, M., & Theeuwes, J. (2011). Feature priming and the capture of visual attention: Linking two ambiguity resolution hypotheses. *Brain research*, *1370*, 175–184. https://doi.org/10.1016/j.brainres.2010.11.025

Hopf, J. M., Boehler, C. N., Luck, S. J., Tsotsos, J. K., Heinze, H. J., & Schoenfeld, M. A. (2006). Direct neurophysiological evidence for spatial suppression surrounding the focus of attention in vision. *Proceedings of the National Academy of Sciences*, *103*(4), 1053–1058. https://doi.org/10.1073/pnas.0507746103

Hopf, J. M., Boehler, C. N., Schoenfeld, M. A., Heinze, H. J., & Tsotsos, J. K. (2010). The spatial profile of the focus of attention in visual search: insights from MEG recordings. *Vision Research*, *50*(14), 1312–1320. https://doi.org/10.1093/cercor/bhn139

Hopf, J. M., Luck, S. J., Girelli, M., Hagner, T., Mangun, G. R., Scheich, H., & Heinze, H. J. (2000). Neural sources of focused attention in visual search. *Cerebral Cortex*, *10*, 1233–1241. https://doi.org/10.1093/cercor/10.12.1233

Hopf, J. M., Vogel, E., Woodman, G., Heinze, H. J., & Luck, S. J. (2002). Localizing visual discrimination processes in time and space. *Journal of Neurophysiology*, *88*, 2088–2095. https://doi.org/10.1152/jn.2002.88.4.2088

Itti, L., & Koch, C. (2000). A saliency-based search mechanism for overt and covert shifts of visual attention. *Vision Research*, *40*, 1489–1506. https://doi.org/10.1016/S0042-6989(99)00163-7

Itti, L., & Koch, C. (2001). Computational modelling of visual attention. *Nature Reviews Neuroscience*, *2*, 194–203. https://doi.org/10.1038/35058500

Jannati, A., Gaspar, J. M., & McDonald, J. J. (2013). Tracking target and distractor processing in fixed-feature visual search: evidence from human electrophysiology. *Journal of Experimental Psychology: Human Perception and Performance*, *39*(6), 1713–1730. https://doi.org/10.1037/a0032251

Jolicoeur, P., Brisson, B., & Robitaille, N. (2008). Dissociation of the N2pc and sustained posterior contralateral negativity in a choice response task. *Brain Research*, *1215*, 160–172. https://doi.org/10.1016/j.brainres.2008.03.059

Joseph, J. S., Chun, M. M., & Nakayama, K. (1997). Attentional requirements in a 'preattentive' feature search task. *Nature*, *387*(6635), 805–807. https://doi.org/10.1038/42940

Julesz, B. (1986). Texton gradients: The texton theory revisited. *Biological Cybernetics*, *54*, 245–251. https://doi.org/10.1007/BF00318420

Kiesel, A., Miller, J., Jolicœur, P., & Brisson, B. (2008). Measurement of ERP latency differences: A comparison of single-participant and jackknife-based scoring methods. *Psychophysiology*, *45*(2), 250–274. https://doi.org/10.1111/j.1469-8986.2007.00618.x

Kiss, M., Van Velzen, J., & Eimer, M. (2008). The N2pc component and its links to attention shifts and spatially selective visual processing. *Psychophysiology*, *45*(2), 240–249. https://doi.org/10.1111/j.1469-8986.2007.00611.x

LaBerge, D. (1995). *Attentional processing: The brain's art of mindfulness.* Harvard University Press. https://doi.org/10.4159/harvard.9780674183940

Leber, A. B., & Egeth, H. E. (2006). It's under control: Top-down search strategies can override attentional capture. *Psychonomic Bulletin & Review*, *13*, 132–138. https://doi.org/10.3758/BF03193824

Logan, G. D. (1988). Toward an instance theory of automatization. *Psychological Review*, *95*, 492–527. https://doi.org/10.1037/0033-295X.95.4.492

Luck, S. J. (2012). Electrophysiological correlates of the focusing of attention within complex visual scenes: N2pc and related ERP components. In S. J. Luck, & E. S. Kappenman (Eds.), The Oxford handbook of event-related potential components (pp. 329–360).

Oxford, UK: Oxford University Press. https://doi.org/10.1093/oxfordhb/9780195374148.001.0001

Luck, S. J., & Ford, M. A. (1998). On the role of selective attention in visual perception. *Proceedings of the National Academy of Sciences*, *95*, 825–830. https://doi.org/10.1073/pnas.95.3.825

Luck, S. J., Girelli, M., McDermott, M. T., & Ford, M. A. (1997). Bridging the gap between monkey neurophysiology and human perception: An ambiguity resolution theory of visual selective attention. *Cognitive Psychology*, *33*, 64–87. https://doi.org/10.1006/cogp.1997.0660

Luck, S. J., & Hillyard, S. A. (1990). Electrophysiological evidence for parallel and serial processing during visual search. *Perception & Psychophysics*, *48*(6), 603–617. https://doi.org/10.3758/BF03211606

Luck, S. J., & Hillyard, S. A. (1994a). Electrophysiological correlates of feature analysis during visual search. *Psychophysiology*, *31*, 291–308. https://doi.org/10.1111/j.1469-8986.1994.tb02218.x

Luck, S. J., & Hillyard, S. A. (1994b). Spatial filtering during visual search: Evidence from human electrophysiology. *Journal of Experimental Psychology Human Perception and Performance*, *20*, 1000–1014. https://doi.org/10.1037/0096-1523.20.5.1000

Mazza, V., & Caramazza, A. (2011). Temporal brain dynamics of multiple object processing: The flexibility of individuation. *PloS one*, *6*(2), e17453. https://doi.org/10.1371/journal.pone.0017453

Mazza, V., & Caramazza, A. (2015). Multiple object individuation and subitizing in enumeration: a view from electrophysiology. *Frontiers in Human Neuroscience*, *9*, 162. https://doi.org/10.3389/fnhum.2015.00162

Mazza, V., Turatto, M., & Caramazza, A. (2009a). An electrophysiological assessment of distractor suppression in visual search tasks. *Psychophysiology*, *46*, 771–775. https://doi.org/ 10.1111/j.1469-8986.2009.00814.x

Mazza, V., Turatto, M., & Caramazza, A. (2009b). Attention selection, distractor suppression and N2pc. *Cortex*, *45*, 879–890. https://doi.org/10.1016/j.cortex.2008.10.009

McDonald, J. J., Green, J. J., Jannati, A., & Di Lollo, V. (2013). On the electrophysiological evidence for the capture of visual attention. *Journal of Experimental Psychology: Human Perception and Performance*, *39*(3), 849–860. https://doi.org/10.1037/a0030510

McDonald, J. J., Tay, D., Prime, D. J., & Hillyard, S. A. (2022). Isolating the neural substrates of visually guided attention orienting in humans. *Journal of Neuroscience*, *42*(20), 4174–4186. https://doi.org/10.1523/JNEUROSCI.0205-22.2022

Miller, J., Patterson, T. U. I., & Ulrich, R. (1998). Jackknife-based method for measuring LRP onset latency differences. *Psychophysiology*, *35*, 99–115. https://doi.org/10.1111/1469-8986.3510099

Neisser, U. (1967). Cognitive psychology. East Norwalk, CT: Appleton-Century-Crofts.

Oostenveld, R., Stegeman, D. F., Praamstra, P., & van Oosterom, A. (2003). Brain symmetry and topographic analysis of lateralized event-related potentials. *Clinical Neurophysiology*, *114*(7), 1194–1202. https://doi.org/10.1016/S1388-2457(03)00059-2

Perrin, F., Pernier, J., Bertrand, O., & Echallier, J. F. (1989). Spherical splines for scalp potential and current density mapping. *Electroencephalography and Clinical Neurophysiology*, *72*, 184–187. https://doi.org/10.1016/0013-4694(89)90180-6

Pitts, M. A., Padwal, J., Fennelly, D., Martínez, A., & Hillyard, S. A. (2014). Gamma band activity and the P3 reflect post-perceptual processes, not visual awareness. *Neuroimage*, *101*, 337–350. https://doi.org/10.1016/j.neuroimage.2014.07.024

Sagi, D., & Julesz, B. (1987). Short-range limitation on detection of feature differences. *Spatial Vision*, *2*, 39–49. https://doi.org/10.1163/156856887X00042

Sawaki, R., Geng, J. J., & Luck, S. J. (2012). A common neural mechanism for preventing and terminating the allocation of attention. *Journal of Neuroscience*, *32*(31), 10725–10736. https://doi.org/10.1523/JNEUROSCI.1864-12.2012

Schneider, W., & Shiffrin, R. M. (1977). Controlled and automatic human information processing: I. Detection, search, and attention. *Psychological Review*, *84*(1), 1–66. https://doi.org/10.1037/0033-295X.84.1.1

Schubö, A., & Müller, H. J. (2009). Selecting and ignoring salient objects within and across dimensions in visual search. *Brain Research*, *1283*, 84–101. https://doi.org/10.1016/j.brainres.2009.05.077

Schubö, A., Schröger, E., & Meinecke, C. (2004). Texture segmentation and visual search for pop-out targets: An ERP study. *Cognitive Brain Research*, *21*, 317–334. https://doi.org/10.1016/j.cogbrainres.2004.06.007

Smulders, F. T. (2010). Simplifying jackknifing of ERPs and getting more out of it: retrieving estimates of participants' latencies. Psychophysiology, 47(2), 387–392. https://doi.org/10.1111/j.1469-8986.2009.00934.x

Tay, D., Harms, V., Hillyard, S. A., & McDonald, J. J. (2019). Electrophysiological correlates of visual singleton detection. *Psychophysiology*, *56*, e13375. https://doi.org/10.1111/psyp.13375

Tay, D., Jannati, A., Green, J. J., & McDonald, J. J. (2022). Dynamic inhibitory control prevents salience-driven capture of visual attention. *Journal of Experimental Psychology: Human Perception and Performance*, *48*, 37 –51. https://doi.org/10.1037/xhp0000972

Theeuwes, J. (1991). Cross-dimensional perceptual selectivity. *Perception & Psychophysics*, *50*, 184–193. https://doi.org/10.3758/BF03212219

Theeuwes, J. (1992). Perceptual selectivity for color and form. *Perception & Psychophysics*, *51*, 599–606. https://doi.org/10.3758/BF03211656

Theeuwes, J. (2010). Top–down and bottom–up control of visual selection. *Acta Psychologica, 35*, 77–99. https://doi.org/10.1016/j.actpsy.2010.02.006

Treisman, A. (1985). Preattentive processing in vision. *Computer Vision, Graphics, and Image Processing*, *31*(2), 156–177. https://doi.org/10.1016/S0734-189X(85)80004-9

Treisman, A. M., & Gelade, G. (1980). A feature-integration theory of attention. *Cognitive Psychology*, *12*, 97–136. https://doi.org/10.1016/0010-0285(80)90005-5

Treisman, A., & Gormican, S. (1988). Feature analysis in early vision: Evidence from search asymmetries. *Psychological Review*, *95*(1), 15–48. https://doi.org/10.1037/0033-295X.95.1.15

Tsotsos, J. K., Culhane, S. M., Wai, W. Y. K., Lai, Y., Davis, N., & Nuflo, F. (1995). Modeling visual attention via selective tuning. *Artificial Intelligence*, *78*(1-2), 507–545. https://doi.org/10.1016/0004-3702(95)00025-9

van Moorselaar, D., Daneshtalab, N., & Slagter, H. A. (2021). Neural mechanisms underlying distractor inhibition on the basis of feature and/or spatial expectations. *Cortex*, *137*, 232–250. https://doi.org/10.1016/j.cortex.2021.01.010

Vogel, E. K., & Machizawa, M. G. (2004). Neural activity predicts individual differences in visual working memory capacity. *Nature*, *428*(6984), 748–751. https://doi.org/ 10.1038/nature02447

Wijers, A. A., Lange, J. J., Mulder, G., & Mulder, L. J. (1997). An ERP study of visual spatial attention and letter target detection for isoluminant and nonisoluminant stimuli. *Psychophysiology*, *34*, 553–565. https://doi.org/ 10.1111/j.1469-8986.1997.tb01742.x

Wolfe, J. M. (1992). “Effortless” texture segmentation and “parallel” visual search are not the same thing. *Vision Research*, *32*, 757–763. https://doi.org/10.1016/0042-6989(92)90190-T

Wolfe, J. M. (1994). Guided search 2.0 a revised model of visual search. *Psychonomic Bulletin & Review*, *1*, 202–238. https://doi.org/10.3758/BF03200774

Woodman, G. F., & Luck, S. J. (1999). Electrophysiological measurement of rapid shifts of attention during visual search. *Nature*, *400*(6747), 867–869. https://doi.org/10.1038/23698

Woodman, G. F., Luck, S. J., & Schall, J. D. (2007). The role of working memory representations in the control of attention. *Cerebral Cortex*, *17*, i118–i124. https://doi.org/10.1093/cercor/bhm065

Wyble, B., Callahan-Flintoft, C., Chen, H., Marinov, T., Sarkar, A., & Bowman, H. (2020). Understanding visual attention with RAGNAROC: A reflexive attention gradient through

996 neural AttRactOr competition. *Psychological Review*, *127*(6), 1163–1198.
997 https://doi.org/10.1037/rev0000245
998 Zivony, A., Allon, A. S., Luria, R., & Lamy, D. (2018). Dissociating between the N2pc and
999 attentional shifting: An attentional blink study. *Neuropsychologia*, *121*, 153–163.
1000 https://doi.org/10.1016/j.neuropsychologia.2018.11.003

Data Availability Statement: Data and materials are available upon request.

Author Contributions: Daniel Tay: conceptualization, formal analysis, investigation, methodology, project administration, software, visualization, writing – original draft preparation. David L. McIntyre: conceptualization, investigation, writing – review and editing. John J. McDonald: conceptualization, formal analysis, funding acquisition, methodology, software, supervision, visualization, writing – original draft preparation.

Acknowledgements: We thank Amanda Klassen, Tristan Khan, Jav Kinger, Brian Mulvany for assistance in data collection.

Funding Information: This study was supported by the Natural Sciences and Engineering Research Council of Canada, the Canadian Foundation for Innovation, and the Canada Research Chairs program. The authors declare no competing financial interest.

Figure Captions

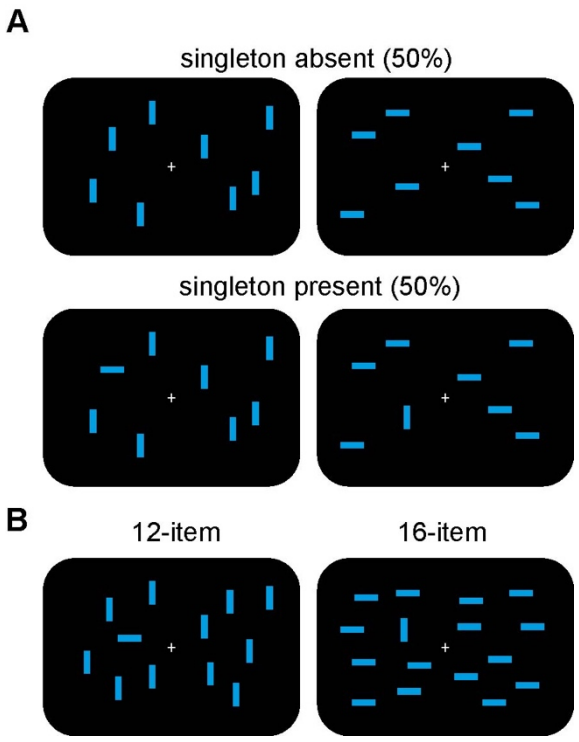

Fig. 1. Example stimulus displays used in Experiment 1 (8-, 12-, and 16-item displays) and Experiment 2 (16-item displays only). (**A**) Eight-item singleton-absent and singleton-present displays. Orientation of the items changed randomly across trials to prevent the adoption of a feature-based search mode. (**B**) Twelve- and 16-item singleton-present displays. Note that half of the 12- and 16-item displays contained no singleton, as in panel (**A**).

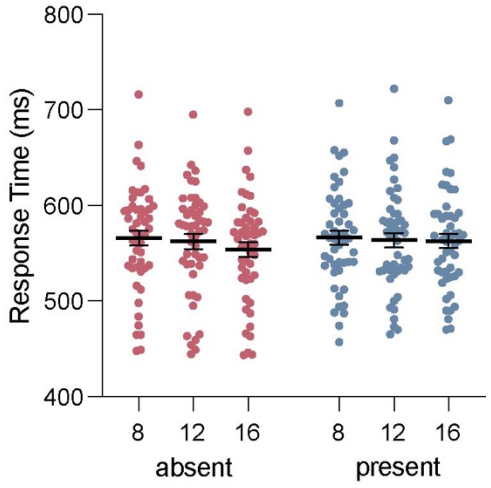

Fig. 2. Behavioural results from Experiment 1. Coloured dots show mean response times (RTs) of individual participants. Thick horizontal lines with SEM bars show the mean RTs across participants as a function of singleton presence and set size.

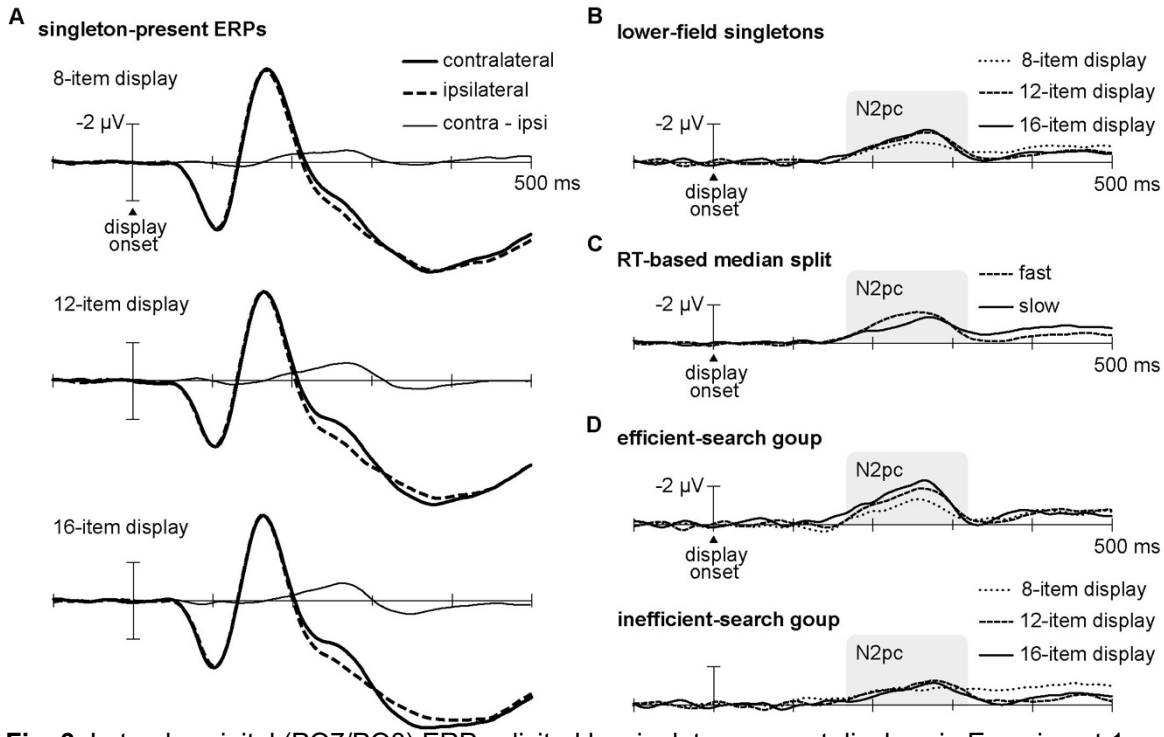

Fig. 3. Lateral occipital (PO7/PO8) ERPs elicited by singleton-present displays in Experiment 1, plotted separately for 8-, 12-, and 16-item set sizes. Negative voltages are plotted upward by convention. (**A**) ERPs recorded contralaterally and ipsilaterally with respect to the position of the singleton (upper or lower left; upper or lower right). The contralateral-minus-ipsilateral difference waveforms are superimposed to show the N2pc components. (**B**) Contralateral-minus-ipsilateral difference waveforms elicited by singletons in the lower field, where N2pc is known to be largest. (**C**) Contralateral-minus-ipsilateral difference waveforms plotted separately for fast-response and slow-response trials based on the median RTs of individual participants. (**D**) Contralateral-minus-ipsilateral difference waveforms plotted separately for efficient-search group and inefficient-search group.

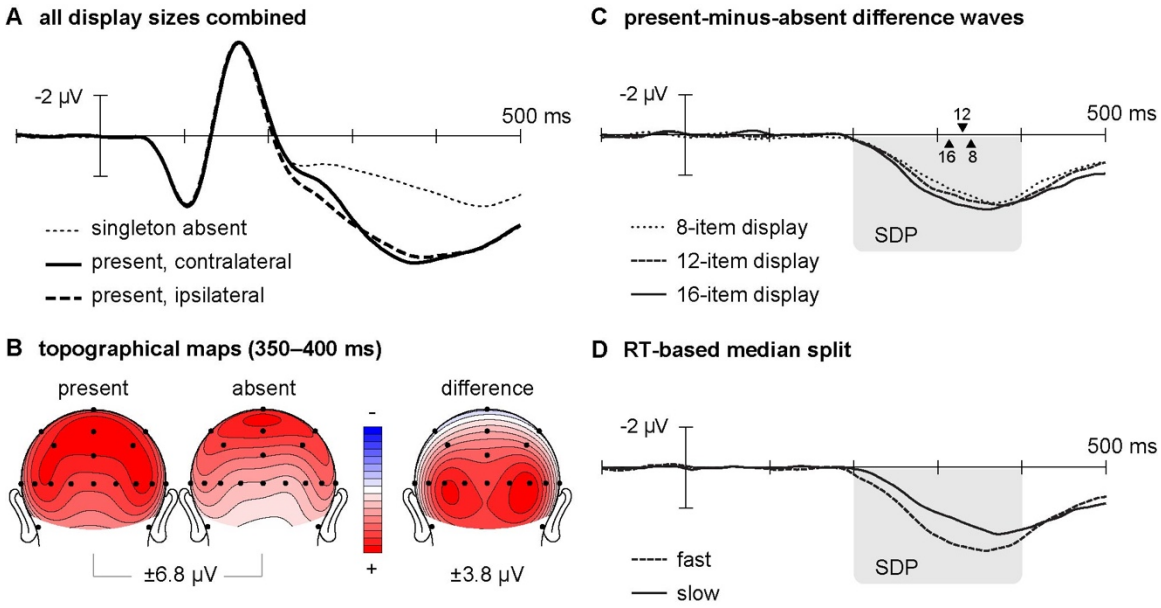

Fig. 4. Isolation of the singleton detection positivity (SDP) in Experiment 1. (**A**) Lateral occipital (PO7/PO8) ERPs elicited by singleton-present and singleton-absent displays, collapsed across all set sizes. The N2pc is evident as the difference between contralateral and ipsilateral waveforms, and the SDP is evident as the difference between either singleton-present waveform and the singleton-absent waveform. (**B**) Topographic maps of the mean voltages within the time range of the SDP for singleton-present displays (left), singleton-absent displays (middle), and the singleton-present-minus-absent difference waveforms (right). (**C**) Ipsilateral singleton-present-minus-absent difference waveforms plotted separately for 8-, 12-, and 16-item displays. Triangles along the abscissa show the 90% fractional peak latencies of the SDP for the three set sizes. (**D**) Ipsilateral singleton-present-minus-absent difference waveforms plotted separately for fast-response and slow-response trials based on the median RTs of individual participants.

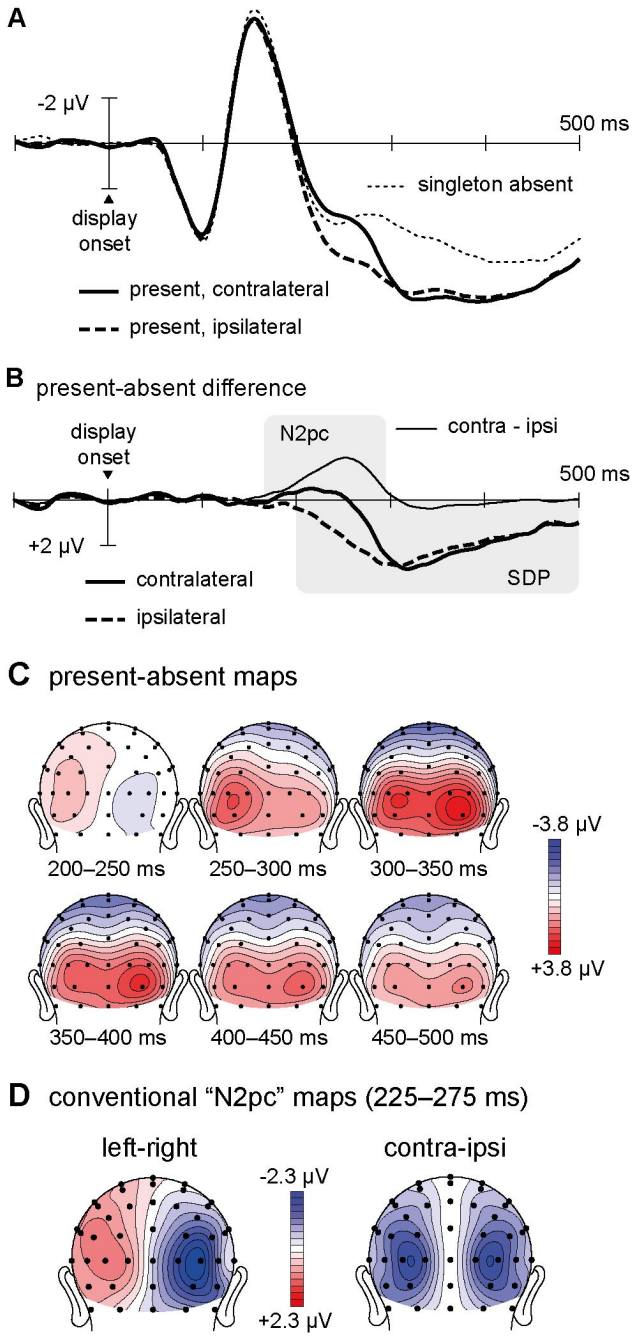

Fig. 5. ERPs elicited by singletons in Experiment 2. (**A**) Grand-averaged ERPs to singleton-present and singleton-absent displays, recorded at lateral occipital electrodes PO7/PO8. (**B**) Present-absent difference waveforms recorded at contralateral and ipsilateral occipital recording sites (PO7/PO8) with the corresponding contralateral-ipsilateral difference wave. (**C**) Topographical maps of mean voltages from the present-absent difference waveforms. The maps were constructed with ipsilateral and contralateral electrodes on the left and right sides of the head, respectively. An averaged mastoid common reference was used for mapping. (**D**) Two methods used previously for estimating the scalp topography of the N2pc: Left-right difference-wave mapping (left) and mirror-symmetric mapping based on contralateral-ipsilateral difference (right).

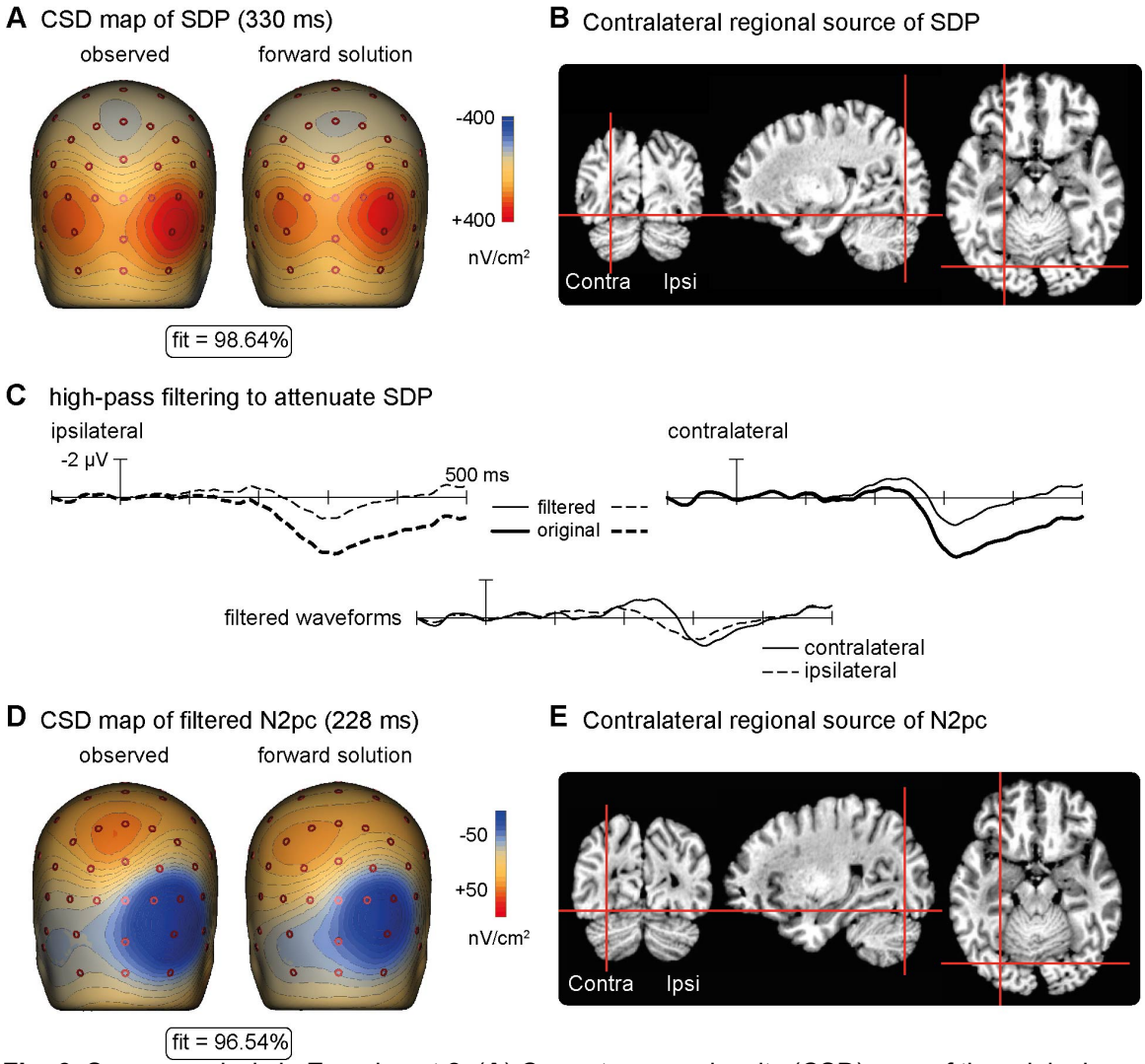

Fig. 6. Source analysis in Experiment 2. (**A**) Current source density (CSD) map of the original present-absent difference waves at best-fitting SDP latency (330 ms), together with the forward solution based on the best-fitting regional source model. The model accounted for over 98.6% of the variance at this time point. (**B**) Coordinates of the contralateral SDP regional source overlaid on anatomical images of the MNI (Colin) brain. SDP sources were situated in Brodmann area 19 (visual association area) near the ventral surface of occipital cortex. (**C**) Effects of the high-pass filter used to attenuate the SDP and to better isolate the N2pc. The original ERPs and the filtered ERPs are overlaid separately for contralateral and ipsilateral electrodes, and then the filtered ERPs are replotted below for visual comparison with the original present-absent difference waveforms in Figure 5B. (**D**) CSD map of the filtered present-absent difference waves in the time range of the N2pc (228 ms), together with the forward solution based on the best-fitting regional source model. The model accounted for over 96.5% of the variance at this time point. (**E**) Coordinates of the contralateral N2pc regional source overlaid on anatomical images of the MNI (Colin) brain. The source was situated in Brodmann area 19 (visual association area) near the ventral surface of occipital cortex.